

# Anisotropic $s$ -wave superconductivity: comparison with experiments on $\text{MgB}_2$ single crystals

A. I. POSAZHENNIKOVA<sup>1,2</sup>, T. DAHM<sup>3,4</sup>, K. MAKI<sup>4,5</sup>

<sup>1</sup> *Laboratorium voor Vaste-Stoffisica en Magnetisme, Katholieke Universiteit Leuven, B-3001 Leuven, Belgium*

<sup>2</sup> *Max-Planck-Institute for the Chemical Physics of Solids, Nöthnitzer Str. 40, D-01187 Dresden, Germany*

<sup>3</sup> *Universität Tübingen, Institut für Theoretische Physik, Auf der Morgenstelle 14, 72076 Tübingen, Germany*

<sup>4</sup> *Max-Planck-Institute for Physics of Complex Systems, Nöthnitzer Str. 38, D-01187 Dresden, Germany*

<sup>5</sup> *Department of Physics and Astronomy, University of Southern California, Los Angeles, CA 90089-0484, USA*

PACS. 74.20.Rp – Pairing symmetries.

PACS. 74.25.Bt – Thermodynamic properties.

PACS. 74.70.Ad – Metals, alloys and binary compounds.

**Abstract.** – The recently discovered superconductivity in  $\text{MgB}_2$  has captured world attention due to its simple crystal structure and relatively high superconducting transition temperature  $T_c = 39\text{K}$ . It appears to be generally accepted that it is phonon-mediated  $s$ -wave BCS like superconductivity. Surprisingly, the strongly temperature dependent anisotropy of the upper critical field, observed experimentally in magnesium diboride single crystals, is still lacking a consistent theoretical explanation. We propose a simple single-gap anisotropic  $s$ -wave order parameter in order to compare its implications with the predictions of a multi-gap isotropic  $s$ -wave model. The quasiparticle density of states, thermodynamic properties, NMR spin-lattice relaxation rate, optical conductivity, and  $H_{c2}$  anisotropy have been analyzed within this anisotropic  $s$ -wave model. We show that the present model can capture many aspects of the unusual superconducting properties of the  $\text{MgB}_2$  compound, though more experimental data appear to be necessary from single crystal  $\text{MgB}_2$ .

*Introduction.* – The moderately high temperature superconductivity with  $T_c \simeq 40\text{K}$ , discovered about one year ago in  $\text{MgB}_2$  [1, 2] has stimulated an intense research activity all over the world. Superconductivity in this binary compound appears to be due to an electron-phonon interaction and compatible with BCS  $s$ -wave superconductivity. Thermodynamics and contact tunneling data as well as some theoretical studies indicate that superconductivity in  $\text{MgB}_2$  is one of the rare examples of two-band superconductivity with two energy gaps, attached to different sheets of the Fermi surface [3–10]. On the other hand, the two gap model appears not to be able to cope with a strongly anisotropic upper critical field in  $c$ -axis oriented  $\text{MgB}_2$  films and more recently in single crystals of  $\text{MgB}_2$  [11–16]. Indeed, the

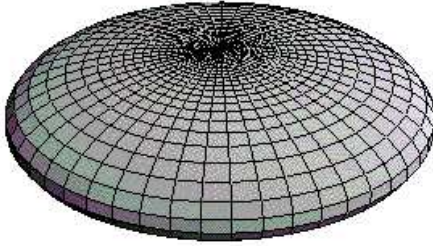


Fig. 1

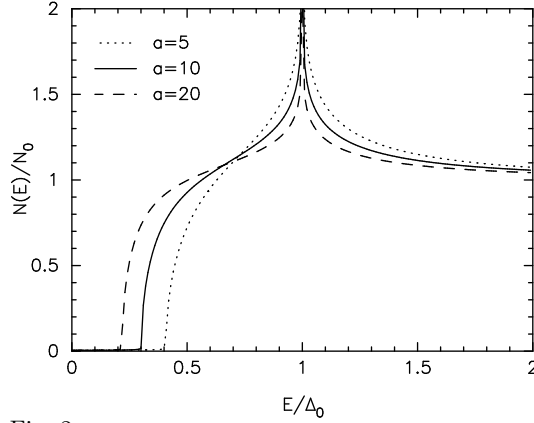


Fig. 2

Fig. 1 – Anisotropic  $s$ -wave order parameter Eq. (1) for  $a = 10$ Fig. 2 – Density of states for  $a = 5, 10$ , and  $20$ .

anisotropic  $s$ -wave model can describe in principle an anisotropy of the upper critical field and an angular dependence of  $H_{c2}$  including deviations from the Ginzburg-Landau prediction with anisotropic mass term [17, 18]. Indeed, some of the STM data appear to be more consistent with an anisotropic  $s$ -wave model [19]. However, more telling is the temperature dependence of the ratio of  $H_{c2}^a(t)$  ( $t \equiv T/T_c$ ) and  $H_{c2}^c(t)$  where the superfix  $a$  and  $c$  denotes a field oriented parallel to the  $a$ -axis or the  $c$ -axis, respectively. The ratio  $\gamma(t) (\equiv H_{c2}^a/H_{c2}^c)$  increases as temperature decreases as has been observed in Refs. [12–14]. This clearly indicates that  $\Delta(\mathbf{k})$  has to have oblate rather than the prolate form suggested earlier [17, 18]. Otherwise  $\gamma(t)$  would decrease with decreasing temperature.

The object of this paper is to propose an oblate  $\Delta(\mathbf{k})$  gap anisotropy and to see whether this order parameter can describe the two gap features observed experimentally. Indeed choosing one adjustable parameter, which determines the ratio of  $\Delta_{\min}/\Delta_{\max}$ , we can describe reasonably well the density of states measured by STM [19] and the specific heat data of Wang et al [4]. Also some peculiarities of the NMR relaxation rate and optical conductivity can be described. Then we shall go on to study the upper critical field for  $\mathbf{H} \parallel \mathbf{c}$  and  $\mathbf{H} \parallel \mathbf{a}$ .

As we shall see later, we can describe  $H_{c2}^c(t)$  reasonably well by choosing our parameter  $a > 5$  (corresponding to a ratio of  $\Delta_{\min}/\Delta_{\max} < 0.4$ , see below). On the other hand, the strong increase of  $H_{c2}^a(t)$  appears to be somewhat difficult to fit consistently with other experimental data within our model. Of course in the real single crystals the electronic mean free path is rather short  $l \simeq 60 \sim 70 \text{ \AA}$  [12–14, 21, 22]. Therefore in a more realistic analysis it is necessary to consider impurity scattering as well.

*Thermodynamics.* – We consider an anisotropic BCS model for superconductivity in  $\text{MgB}_2$  with an order parameter given by

$$\Delta(\mathbf{k}) = \Delta \frac{1}{\sqrt{1 + az^2}}, \quad (1)$$

where the parameter  $a$  determines the anisotropy,  $z = \cos(\theta)$  and  $\theta$  is the polar angle with respect to the  $c$ -axis. In Fig. 1 the anisotropic  $s$ -wave order parameter is plotted in momentum

TABLE I – Gap ratios and specific heat jumps for  $a = 5, 10, 20$ , and  $40$ .

$a$	$\frac{\Delta_{\max}}{T_c}$	$\frac{\Delta_{\min}}{T_c}$	$\frac{\Delta C}{\gamma T_c}$
5	2.29	0.93	1.11
10	2.46	0.74	0.93
20	2.61	0.57	0.74
40	2.78	0.43	0.57

space for  $a = 10$  displaying a pancake-like shape. Its maximum value  $\Delta_{\max} = \Delta$  lies in the  $ab$ -plane, while in  $c$ -axis direction it assumes its minimum value of  $\Delta_{\min} = \Delta/\sqrt{1+a}$ . In the following we will explore the consequences of anisotropic  $s$ -wave superconductivity in  $\text{MgB}_2$  within the framework of the weak-coupling BCS theory.

We have solved numerically the weak-coupling gap equation for the state Eq. (1)

$$\int_0^\infty d\epsilon \left\{ \langle f^2(z) \rangle^{-1} \left\langle \frac{f^2(z)}{\sqrt{\epsilon^2 + \Delta^2 f^2(z)}} \tanh \left( \frac{\sqrt{\epsilon^2 + \Delta^2 f^2(z)}}{2T} \right) \right\rangle - \frac{1}{\epsilon} \tanh \left( \frac{\epsilon}{2T_c} \right) \right\} = 0 \quad (2)$$

Here,  $f(z) = 1/\sqrt{1+az^2}$  and  $\langle \dots \rangle = \int_0^1 dz \dots$  denotes an angular average over the variable  $z$ . In Table I we tabulated gap ratios found from the solution of Eq. (2) for  $a = 5, 10, 20$ , and  $40$ . With increasing value of  $a$  an increasing gap ratio of the maximum gap  $\Delta_{\max}/T_c$  is found, while the minimum gap ratio appears to decrease.

In Fig. 2 we show the corresponding density of states for these values of  $a$  calculated from

$$N(E)/N_0 = \text{Re} \left\langle \frac{E}{\sqrt{E^2 - \Delta^2 f^2(z)}} \right\rangle \quad (3)$$

The data in [19] resembles our density of states if we choose  $a \sim 3$ . Further the peak in the density of states in [19] gives a maximum gap  $\sim 8$  meV consistent with our model. Also the authors [19] deduced a momentum dependence of  $\Delta(\mathbf{k})$ , which is topologically the same as the earlier model [17,18]. On the other hand, the data in [20] exhibits a two gap like structure very different from Fig. 2. Further, the maximum gap 7 meV is somewhat smaller than the one expected from the present model. However, the double gap like feature is inherent to the anisotropic gap, since the two extrema associated with the single gap are always visible [17,18].

In Fig. 3 the specific heat is shown for values of  $a = 10, 20$ , and  $40$  along with the data of Wang et al. [4,5]. The specific heat jumps found from our model are also tabulated in Table I. They decrease with increasing  $a$ . The closest agreement with the experimental data is obtained for  $a = 20$ . However, fitting of the structures seen in the experimental data would require some fine tuning of the angular dependence in Eq. (1).

In Fig. 4 we show the normalized NMR spin-lattice relaxation rate obtained from our state. With increasing anisotropy  $a$  the Hebel-Slichter peak is reduced. Roughly, the size of the peak found here is consistent with recent NMR data on polycrystalline  $\text{MgB}_2$  by Kotegawa et al. [23].

It has recently been noted that the gap seen in optical conductivity appears to be very small [24,25]. We calculated the anisotropic analog of the Mattis-Bardeen conductivity [26] averaged over all directions, which should correspond to the response of a polycrystalline thin film sample as has been used in Refs. [24,25]. For our anisotropic state the conductivity  $\sigma(\omega)$  is obtained using the following two functions:

$$I_1(x) = \int_0^1 dz \int_{f(z)}^\infty dy \frac{f^2(z) + y(y+x)}{\sqrt{(y^2 - f^2(z))[(y+x)^2 - f^2(z)]}} \left[ \tanh \left( \frac{(x+y)\Delta}{2T} \right) - \tanh \left( \frac{y\Delta}{2T} \right) \right]$$

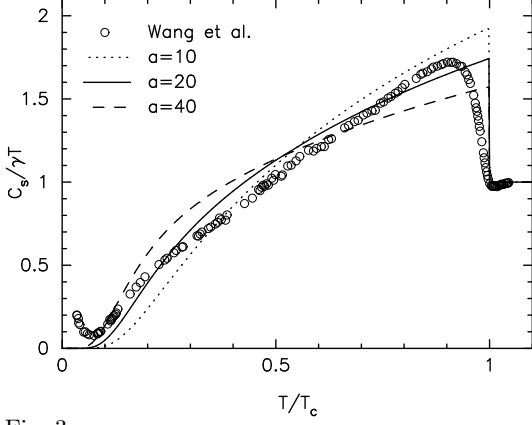


Fig. 3

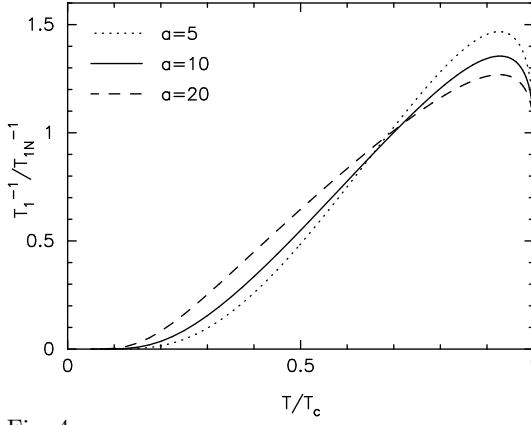


Fig. 4

Fig. 3 – Reduced specific heat  $C/\gamma T$  for  $a=10, 20$ , and  $40$ . The symbols are data from Ref. [4].Fig. 4 – Normalized NMR spin-lattice relaxation rate  $T_1^{-1}/T_{1N}^{-1}$  for  $a=5, 10$ , and  $20$ .

$$I_2(x, z_0) = \int_{z_0}^1 dz \int_{f(z)}^\infty dy \frac{f^2(z) - y(x-y)}{\sqrt{(y^2 - f^2(z))[(y-x)^2 - f^2(z)]}} \tanh\left(\frac{y\Delta}{2T}\right)$$

Using these the optical conductivity reads

$$\frac{\sigma(\omega)}{\sigma_N} = \begin{cases} \frac{\Delta}{\omega} I_1\left(\frac{\omega}{\Delta}\right) & \text{for } \omega < 2\Delta_{\min} \\ \frac{\Delta}{\omega} \left[ I_1\left(\frac{\omega}{\Delta}\right) - I_2\left(\frac{\omega}{\Delta}, \sqrt{\frac{4\Delta^2 - \omega^2}{a\omega^2}}\right) \right] & \text{for } 2\Delta_{\min} < \omega < 2\Delta_{\max} \\ \frac{\Delta}{\omega} [I_1\left(\frac{\omega}{\Delta}\right) - I_2\left(\frac{\omega}{\Delta}, 0\right)] & \text{for } \omega > 2\Delta_{\max} \end{cases} \quad (4)$$

The result for  $a=20$  and different reduced temperatures is shown in Fig. 5. Indeed it appears that the optical conductivity is mainly dominated by the minimum gap within our model, because the absorption threshold starts at  $2\Delta_{\min}$ . Thus, an anisotropic gap scenario can also account for the small gap seen in the optical conductivity. Most useful would be optical conductivity studies on single crystals which could resolve the  $c$ -axis and  $ab$ -plane response in order to see more clearly, what the anisotropy looks like.

*Upper critical field.* – Recent experiments on the upper critical field in  $\text{MgB}_2$  single crystals have reported a strong temperature dependent anisotropy of  $H_{c2}$  and an unusual upward curvature of the critical field parallel to the  $ab$  plane. An anisotropy of the superconducting pairing can in principle give such an effect. We investigate the temperature dependence of both  $H_{c2}$ , parallel and perpendicular to the crystal  $c$ -axis of  $\text{MgB}_2$ .

The general equation for the upper critical field is derived from the gap equation. For unconventional superconductors it can be treated variationally, some technical details can be found elsewhere [27].

(a)  $\mathbf{H} \parallel \mathbf{c}$

The equation for the upper critical field parallel to the  $c$ -axis is given by

$$-\ln t = \int_0^\infty \frac{du}{\sinh u} \left( 1 - \langle f^2 \rangle^{-1} \left\langle \exp(-\rho u^2(1-z^2)) f^2 \right\rangle \right), \quad (5)$$

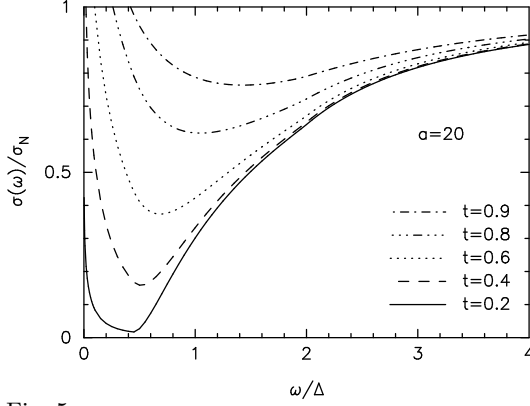


Fig. 5

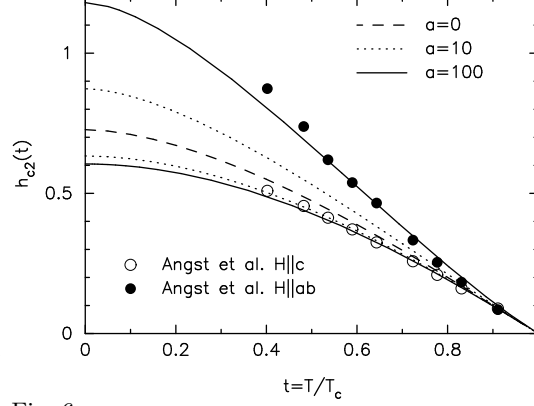


Fig. 6

Fig. 5 – Mattis-Bardeen conductivity as a function of normalized frequency  $\omega/\Delta$  for  $a = 20$  and reduced temperatures  $t = T/T_c$  of 0.9, 0.8, 0.6, 0.4, and 0.2 (from top to bottom), respectively.

Fig. 6 – Normalized upper critical field  $h_{c2}$  as a function of reduced temperature  $t$  for  $a = 10$  and  $a = 100$ . The upper two curves are for field direction within the  $ab$ -plane, while the lower two curves are for field in  $c$ -axis direction. For comparison also the isotropic result ( $a = 0$ ) is shown. The data points are taken from Ref. [13], where we have normalized them to the slope at  $T_c$ , taking  $T_c = 37.3\text{K}$ ,  $\frac{dH_{c2,ab}}{dT}|_{T_c} \simeq -0.435\text{T/K}$ , and  $\frac{dH_{c2,c}}{dT}|_{T_c} \simeq -0.124\text{T/K}$ .

where  $\rho = v_a^2 e H_{c2}(t) / (2\pi T)^2$ , and  $v_a$  is the Fermi velocity within the  $ab$ -plane.

In Fig. 6 the numerical solution of this equation, normalized by its derivative at  $T_c$ ,  $h_{c2}(T) \equiv H_{c2}(T) / (-T_c \partial H_{c2}(T) / \partial T)|_{T_c}$ , is plotted along with the  $h_{c2}(T)$ -curves for the  $ab$ -direction, the corresponding curve for the isotropic case, and normalized experimental data by Angst et al. [13]. In the limit  $T \rightarrow 0$  for  $a = 10$  we have  $h_{c2}^c(0) \simeq 0.63349$  which is somewhat smaller than the corresponding value in the isotropic  $s$ -wave superconductor  $h_{c2}(0) \simeq 0.72726$ . In the vicinity of  $T_c$  the upper critical field exhibits naturally a rather linear temperature dependence within the weak-coupling BCS theory. This behavior is observed for both anisotropic  $s$ -wave and conventional superconductors. Note, that our results for the upper critical field parallel to the  $c$ -axis for  $a > 5$  are in good correspondence with the experimental data [13]. The best fit to these data is obtained for  $a \approx 10$ . However, we cannot reliably extract a value of  $a$  from these data, because  $h_{c2}^c(0)$  for  $a \rightarrow \infty$  is saturating at a value of 0.59054 and the data are already close to this limit. Thus, also even higher values of  $a$  might still be consistent with the  $c$ -axis data.

#### (b) $\mathbf{H} \parallel \mathbf{a}$

The derivation of the equation for the temperature dependent upper critical field in the plane is more involved. The problem is that a mixing of higher Landau levels takes place [27]. We choose a variational wavefunction suggested in Ref. [28], Eq. (36), which corresponds to a distorted Abrikosov ground state. Due to the anisotropy of our state such a distortion is expected for the field direction perpendicular to the  $c$ -axis. The distortion can be varied using a parameter  $\alpha$ , which has to be determined by a variational principle. Using this method we arrive at the following equation for the temperature dependence of the upper critical field

$$\rho_a(t) = v_a v_c e H_{c2}(t) / 2(2\pi T)^2$$

$$-\ln t = \int_0^\infty \frac{du}{\sinh u} \left\{ 1 - \langle f^2 \rangle^{-1} \left\langle \exp \left\{ -\rho_a u^2 \left( \frac{1}{\alpha^2} (1 - z^2) \cos^2 \phi + \alpha^2 z^2 \right) \right\} f^2 \right\rangle \right\}, \quad (6)$$

here  $\langle \dots \rangle = \int_0^1 dz \int_0^{2\pi} \frac{d\phi}{2\pi} \dots$  and  $v_c$  is the Fermi velocity in  $c$ -axis direction. The parameter  $\alpha$  has to be determined from a minimization of the right-hand side of Eq. (6), taking its derivative to be zero.

We have compared our results with a second, independent calculation based on a Landau level expansion up to the fourth Landau level following the method of Luk'yanchuk and Mineev [29]. For the parameter range  $a < 20$  both methods were in close agreement with each other. However, for  $a \gg 20$  the Landau level expansion started to give significantly smaller values for  $H_{c2}^a$ , indicating that inclusion of even higher Landau levels becomes necessary, and showing that the distorted Abrikosov wavefunction is a better variational solution in this case.

The numerical solution of Eq. (6) obtained from a numerical optimization of  $\alpha$  is shown in Fig. 6. In the zero-temperature limit we obtain  $h_{c2}^a = 0.87309$  for  $a = 10$  and  $h_{c2}^a = 1.18025$  for  $a = 100$ . The curve for  $a = 100$  possesses a slight upward curvature in agreement with the experimental data. From our comparison with the experimental data [13] we extracted the values  $-\partial H_{c2}^a(T)/\partial T \simeq 0.435$  T/K and  $-\partial H_{c2}^c(T)/\partial T \simeq 0.124$  T/K. Choosing  $a = 10$ , from these we deduce average Fermi velocities  $v_a \simeq 2.7 \cdot 10^7$  cm/sec,  $v_c \simeq 1.3 \cdot 10^7$  cm/sec and the ratio  $v_c/v_a \simeq 0.48$ . The last ratio is very consistent with what was obtained earlier [17] using the data in [11]. Also the absolute values of these Fermi velocities  $v_a$  and  $v_c$  are roughly consistent with bandstructure calculation results provided to us by A. Yaresko.

This rather large value of  $a = 100$  appears to give a reasonable fit to the  $ab$ -plane data of  $H_{c2}$ . But unfortunately, this corresponds to a ratio of  $\Delta_{\min}/\Delta_{\max} \simeq 0.1$ , which appears to be inconsistent with the values we discussed above. Here we can just speculate about a possible resolution of this problem: in these single crystals the mean free path is relatively short, being about the order of the coherence length [21, 22], which puts these systems in an intermediate region between the clean and the dirty limit. Therefore a study of the influence of impurity scattering would be necessary. It is possible that the upper critical field anisotropy is much less sensitive to impurity scattering than the energy gap and the density of states, for example. Such an effect could possibly resolve this problem and is left for a future work.

*Conclusions.* – We have described a model of anisotropic s-wave superconductivity and compared our theoretical predictions with the experimental data of MgB<sub>2</sub>. We show that our model can capture many aspects of the two gap model and is consistent with the experimental data of single crystals MgB<sub>2</sub>. Also we stress that so far our model is the only one, that can describe the strongly temperature dependent anisotropy in the upper critical field. Unfortunately, strongly different values of our anisotropy parameter  $a$  had to be used for different experimental properties. On the other hand, we have ignored the effect of impurity scattering in the present analysis. In particular the mean free path  $l \sim 60 - 70 \text{ \AA}$  reported for single crystals of MgB<sub>2</sub> implies that we are in the intermediate regime (neither in the clean limit nor in the dirty limit). Therefore in a more realistic analysis, it will be very important to incorporate the effect of impurity scattering. Clearly, we also need more precise measurements on single crystal MgB<sub>2</sub>.

\*\*\*

We would like to thank M. Angst, F. Bouquet, and A. Junod for providing us with the digital form of their experimental data. Thanks are also due to Y. Takano, J. Karpinski,

P. Thalmeier, A. Yaresko, and N. Schopohl for useful discussions related to this subject. We are indebted to Todor M. Mishonov for pointing out to us an error in Table I in the first version of this manuscript.

## REFERENCES

- [1] J. Nagamatsu, N. Nakagawa, T. Muranaka, Y. Zenitani, J. Akimitsu, *Nature*(London) **410**, 63 (2001).
- [2] C. Buzea and T. Yamashita, *Supercond. Sci. Technol.* **14**, R115 (2001).
- [3] P. Szabo et al., *Phys. Rev. Lett.* **87**, 137005 (2001).
- [4] Y. Wang, T. Plackowski, and A. Junod, *Physica C* **355**, 179 (2001).
- [5] F. Bouquet, Y. Wang, R. A. Fisher, P. G. Hinks, J. D. Jorgensen, A. Junod, and N. E. Phillips, *Europhys. Lett.* **56**, 856 (2001).
- [6] S. V. Shulga, S. L. Drechsler, H. Eschrig, H. Rosner, and W. Pickett, cond-mat/0103154.
- [7] E. Bascones and F. Guinea, *Phys. Rev. B* **64**, 214508 (2001).
- [8] J. M. An and W. E. Pickett, *Phys. Rev. Lett.* **86**, 4366 (2001).
- [9] A. Y. Liu, I. I. Mazin, and J. Kortus, *Phys. Rev. Lett.* **87**, 087005 (2001).
- [10] A. A. Golubov et al., *J. Phys.: Condens. Matter* **14**, 1353 (2002).
- [11] O. F. de Lima et al., *Phys. Rev. B* **64**, 144517 (2001).
- [12] M. Xu, H. Kitazawa, Y. Takano, J. Ye, K. Nishida, H. Abe, A. Matsushita, N. Tsujii and G. Kido, *Appl. Phys. Lett.* **79**, 2779 (2001).
- [13] M. Angst, R. Puzniak, A. Wisniewski, J. Jun, S.M. Kazakov, J. Karpinski, J. Roos, and H. Keller, *Phys. Rev. Lett.* **88**, 167004 (2002).
- [14] A. V. Sologubenko, J. Jun, S. M. Kazakov, J. Karpinski, H. R. Ott, *Phys. Rev. B* **65**, 180505(R) (2002).
- [15] Yu. Eltsev, S. Lee, K. Nakao, N. Chikumoto, S. Tajima, N. Koshizuka, and M. Murakami, *Phys. Rev. B* **65**, 140501(R) (2002); *Physica C* (Proceedings of ISS2001, Kobe, Japan, Sept.24-26, 2001), in press.
- [16] U. Welp, G. Karapetrov, W. K. Kwok, G. W. Crabtree, Ch. Marcenat, L. Paulius, T. Klein, J. Marcus, K. H. P. Kim, C. U. Jung, H.-S. Lee, B. Kang, S.-I. Lee, cond-mat/0203337.
- [17] Y. Chen, S. Haas, and K. Maki, *Current Appl. Phys.* **1**, 333 (2001).
- [18] S. Haas and K. Maki, *Phys. Rev. B* **65**, 020502(R) (2002).
- [19] P. Seneor et al, *Phys. Rev. B* **65**, 012505 (2002).
- [20] F. Giubileo et al, *Phys. Rev. Lett.* **87**, 177008 (2001).
- [21] J. H. Jung et al, *Phys. Rev. B* **65**, 052413 (2002).
- [22] S. Lee, H. Mori, Yu. Eltsev, A. Yamamoto, S. Tajima, *J. Phys. Soc. Jpn.* **70**, 2255 (2001).
- [23] H. Kotegawa, K. Ishida, Y. Kitaoka, T. Muranaka, and J. Akimitsu, *Phys. Rev. Lett.* **87**, 127001 (2001).
- [24] R. A. Kaindl et al, *Phys. Rev. Lett.* **88**, 027003 (2002).
- [25] A. Pimenov, A. Loidl, and S. I. Krasnovobodtsev, *Phys. Rev. B* **65**, 172502 (2002).
- [26] D. C. Mattis and J. Bardeen, *Phys. Rev.* **111**, 412 (1958).
- [27] Y. Sun and K. Maki, *Phys. Rev. B* **47**, 9108 (1993).
- [28] C.T. Rieck, K. Scharnberg, and N. Schopohl, *J. Low Temp. Phys.* **84**, 381 (1991).
- [29] I. A. Luk'yanchuk and V. P. Mineev, *Zh. Eksp. Teor. Fiz.* **93**, 2030 (1987) [*Sov. Phys. JETP* **66**, 1158 (1987)].